



Clinical and Molecular Spectrum of *PIK3CA*-Related Overgrowth Syndrome: A Turkish Cohort

Elifcan Taşdelen¹, Selin Sennaroğlu¹, Abdulkerim Kolkıran², Melike Ataseven Kulalı², İbrahim Kaplan³, Mustafa Tarık Alay¹, Şule Yeşil⁴

1 Department of Medical Genetics, Ankara Etlik City Hospital, Ankara, Türkiye

2 Department of Pediatric Genetics, Ankara Etlik City Hospital, Ankara, Türkiye

3 Department of Medical Genetics, Adana City Hospital, Adana, Türkiye

4 Department of Pediatric Hematology and Oncology, Ankara Etlik City Hospital, Ankara, Türkiye

Received: 26.12.2025; Revised: 18.02.2026; Accepted: 20.02.2026

Abstract

Background: *PIK3CA*-related overgrowth spectrum (PROS) includes a group of mosaic overgrowth disorders caused by postzygotic gain-of-function variants in the *PIK3CA* gene. These variants lead to upregulation of the PI3K/AKT/mTOR signaling pathway, resulting in dysregulated cell growth, proliferation, and vasculogenesis. Disorders such as KTWS and CLOVES syndrome share overlapping clinical features such as segmental overgrowth, vascular and lymphatic malformations, and cutaneous involvement.

Methods: A cohort of five Turkish patients with clinical findings consistent with PROS was evaluated. High-depth next-generation sequencing (NGS) was performed on affected tissue samples, and the identified variants on *PIK3CA* gene were interpreted according to ACMG/AMP criteria. Clinical, radiological, and molecular data were integrated to assess genotype-phenotype correlations.

Results: Five distinct somatic *PIK3CA* variants were identified. Four were in the C-terminal helical and kinase domains—known mutational hotspots—while one variant was found in the N-terminal adaptor-binding (PI3K-ABD) domain. Four variants were missense substitutions, and one was an in-frame deletion. The mean sequencing depth was approximately 1100×, and the lowest variant allele frequency (VAF) detected was 2%. No correlation was observed between VAF and disease severity.

Conclusion: This Turkish cohort highlights the clinical and molecular heterogeneity of PROS and emphasizes the importance of tissue-targeted, high-depth sequencing in detecting low-level mosaic variants. Molecular confirmation of *PIK3CA* mosaicism is essential for accurate diagnosis and therapeutic decision-making. Considering the recent evidence supporting the efficacy of Alpelisib in both pediatric and adult PROS patients, early recognition and molecular characterization of these cases are critical for guiding precision therapy and improving clinical outcomes.

Keywords: *PIK3CA*, overgrowth, segmental, somatic, mosaic

DOI: 10.5798/dicletip.1906487

Correspondence / Yazışma Adresi: Elifcan Taşdelen, Department of Medical Genetics, Ankara Etlik City Hospital Varlık, Ankara, Türkiye e-mail: elifkarakaya2012@gmail.com

PIK3CA-İlişkili Aşırı Büyüme Sendromlarının Klinik ve Moleküler Spektrumu: Türk Hasta Kohortu

Öz

Arka Plan: *PIK3CA*-ilişkili aşırı büyüme spektrumu (PROS), *PIK3CA* geninde postzigotik dönemde ortaya çıkan işlev kazandırıcı ('gain-of-function') varyantlardan kaynaklanan mozaik aşırı büyüme sendromlarını kapsar. Bu varyantlar, PI3K/AKT/mTOR sinyal yolunun aktivasyonuna yol açarak hücre büyümesi, proliferasyonu ve damar gelişiminin düzeninin bozulmasına neden olur. Alt tiplerinden olan KTWS ve CLOVES sendromu gibi tablolar; segmental aşırı büyüme, vasküler ve lenfatik malformasyonlar ile deri tutulumunu içeren örtüşen klinik özellikler gösterir.

Yöntemler: PROS ile uyumlu klinik bulgulara sahip beş Türk hastadan oluşan bir kohort değerlendirildi. Etkilenen doku örneklerinden yüksek derinlikli yeni nesil dizileme (NGS) analizi yapıldı ve saptanan *PIK3CA* gen varyantları ACMG/AMP kriterlerine göre yorumlandı. Klinik, radyolojik ve moleküler veriler entegre edilerek genotip-fenotip ilişkileri incelendi.

Bulgular: Toplam beş farklı somatik *PIK3CA* varyantı tanımlandı. Dördü C-terminal helikal ve kinaz bölgelerinde (bilinen mutasyonel sıcak noktalar), biri ise N-terminal adaptor-bağlanma (PI3K-ABD) bölgesinde yer almaktaydı. Dört varyant 'missense' değişimi, biri ise çerçeve kayması oluşturmeyen ('in-frame') delesyondur. Ortalama dizileme derinliği yaklaşık 1100× olup, saptanan en düşük varyant alel frekansı (VAF) %2 idi. VAF ile hastalık şiddeti arasında belirgin bir ilişki gözlenmedi.

Sonuç: Bu Türk kohortu, PROS'un klinik ve moleküler heterojenitesini vurgulamakta ve düşük düzeydeki mozaik varyantların saptanmasında dokuya özgü, yüksek derinlikli dizilemenin önemini ortaya koymaktadır. *PIK3CA* mozaizminin moleküler olarak doğrulanması, doğru tanı ve uygun tedavi seçimi açısından kritik öneme sahiptir. Hem pediatrik hem de erişkin PROS olgularında Alpelisib tedavisinin etkinliğini destekleyen güncel veriler göz önüne alındığında, bu hastaların erken tanınması ve moleküler olarak karakterize edilmesi, hedefe yönelik tedavi ve klinik sonuçların iyileştirilmesi açısından büyük önem taşımaktadır.

Anahtar kelimeler: *PIK3CA*, aşırı büyüme, segmental, somatik, mozaik.

INTRODUCTION

PIK3CA-related disorders (*PIK3CA*, OMIM: *171834) represent a group of genetic conditions caused by postzygotic somatic mosaic variants in the *PIK3CA* gene, which encodes the catalytic subunit alpha (p110 α) of phosphatidylinositol-3-kinase (PI3K). These disorders are characterized by segmental or regional overgrowth affecting various body parts. The phenotypic spectrum is wide, encompassing multiple overlapping clinical conditions such as Congenital Lipomatous Overgrowth, Vascular malformations, Epidermal nevi, and Spinal or skeletal anomalies and/or scoliosis (CLOVES, #612918); megalencephaly-capillary malformation-polymicrogyria syndrome (MCAP, #602501); Klippel-Trenaunay-Weber syndrome (KTWS) (%149000); epidermal nevus (#162900); and macrodactyly (#155500). These disorders are collectively referred to as the *PIK3CA*-related overgrowth spectrum (PROS)^{1,2}.

The severity of PROS varies considerably, even among individuals with the same genetic alteration, a variability thought to result from differences in the timing of the somatic mutation during embryogenesis and the extent of the affected tissues. Clinically, PROS can involve overgrowth of multiple tissues, including the brain, adipose, vascular, skeletal, muscular, and neural structures. Vascular and lymphatic malformations, cutaneous lesions such as epidermal nevi and hyperpigmented macules, and digital anomalies including macrodactyly, syndactyly, or polydactyly are frequent findings. Brain MRI may reveal hemimegalencephaly, focal cortical dysplasia or dysplastic megalencephaly, while renal malformations and benign overgrowth lesions may also occur³.

Recently, the approval of Alpelisib (VIOICE®), a PI3K inhibitor, by the U.S. Food and Drug Administration (FDA) for the treatment of PROS

has underscored the importance of early and accurate diagnosis of these disorders.

In this study, we present the clinical, radiological and molecular findings of five patients diagnosed with PROS at our tertiary-center, emphasizing the genotype–phenotype correlations and diagnostic challenges associated with this heterogeneous spectrum.

METHODS

Five patients who were followed up at Ankara Etlik City Hospital were included in this study. Written informed consent was obtained from the legal guardians of all participants. For the retrospective analysis of the *PIK3CA* gene, DNA extracted from patients' skin samples obtained from affected areas was analyzed by Next-Generation Sequencing (NGS) using the Seq Genomize v8.2.3 platform (Roche), with library preparation performed using the KAPA HyperCap Custom kit. Variant calls were assessed using stringent criteria, including read depth, variant-supporting read count, quality metrics, and artifact filtering, enabling reliable detection of variants with VAF as low as 2%.

RESULTS

Clinical Findings

Patient 1

A 20-year-old female was evaluated for congenital right-sided overgrowth. There was no parental consanguinity and she had five healthy siblings. Her prenatal, postnatal, and developmental histories were all within normal limits. Since birth, she had been under regular endocrinologic follow-up due to right-sided hemihypertrophy with consistently normal hormonal profiles. On physical examination, she exhibited right-sided overgrowth involving the arm (Fig. 1a), hand, leg, and foot, along with scoliosis. Prominent surface veins (Fig. 1b) were observed on the right leg. Macroductyly of the left second finger and a port-wine stain on the right plantar surface were also noted (Fig.

1c). Abdominal ultrasonography revealed hepatomegaly. Targeted NGS performed on a skin biopsy sample obtained from the overgrown right leg identified a somatic *PIK3CA* variant, c.3129G>T (p.Met1043Ile), with a variant allele frequency (VAF) of 3% and a read depth of 1071 (Fig. 2a). According to ACMG/AMP guidelines, the variant met the criteria PS1, PS3, PM1, PM2, and PM5, and was therefore classified as pathogenic.

Patient 2

A 2-day-old male infant with antenatally diagnosed fetal lymphedema, pleural effusion, and hemangioma was referred to our clinic. He was born at 37 + 5 weeks of gestation via spontaneous vaginal delivery, weighing 3461 grams with a head circumference of 34 cm. After birth, he was admitted to the neonatal intensive care unit for close monitoring. He had one healthy sibling.

Extensive prenatal and postnatal ultrasonographic evaluations—including transabdominal, abdominal, cranial, and thoracic assessments—showed no abnormalities; however, echocardiography identified a secundum atrial septal defect (ASD). On physical examination, facial asymmetry was noted due to a soft, mobile 2 cm mass on the left cheek (Fig. 1d). Additional findings included anteverted nostrils, a flattened nasal bridge, retrognathia, broad plantar surfaces, and caudally positioned thumbs. Multiple cutaneous hemangiomas were observed on the left lateral thorax, back (Fig. 1e), and upper abdomen. Soft-tissue overgrowth with venous prominence was evident on the anterior aspect of the tibia and the left side of the back. Thoracoabdominal MRI demonstrated an extensive multiloculated lymphatic malformation predominantly involving the subcutaneous tissue of the left hemibody, extending from the thoracic wall to the gluteal and proximal thigh regions with minimal intramuscular extension. Targeted NGS performed on affected tissue identified a

somatic *PIK3CA* (NM_006218.4) variant, c.328_330del (p.Glu110del), with a VAF of 5% and a read depth of 836 (Fig. 2b). In accordance with ACMG/AMP guidelines, this in-frame deletion fulfilled the criteria PM1, PM2, PM4, and PS4, leading to its classification as pathogenic. Based on clinical and molecular findings sirolimus therapy was initiated. On post-treatment thoracic MRI, precise measurement of the lesion was not feasible due to its extensive distribution; however, comparison with prior imaging demonstrated a reduction in size.

Patient 3

A 2-year-old female was referred to our clinic for genetic evaluation due to macrodactyly. She was born at 39 + 6 weeks of gestation via spontaneous vaginal delivery, weighing 2900 g, as the second child of non-consanguineous parents from the same village. She had a healthy 5-year-old brother. Prenatal, postnatal, and family histories were all unremarkable. She exhibited mild developmental delay, as she achieved independent sitting at 12 months of age, while other developmental milestones were appropriate for her age. On physical examination, her weight was 9 kg (-2.39 SDS), height was 82 cm (-1.6 SDS), and head circumference was 48 cm (-2.26 SDS). The left fifth finger was elongated, thick, and showed clinodactyly. Additional findings included joint laxity of the lower limbs, pectus excavatum, and soft-tissue hypertrophy posterior aspect of the left shoulder. Investigations including karyotype, chromosomal microarray (CMA), MLPA analysis for Beckwith-Wiedemann syndrome (BWS), echocardiography, electrocardiography and abdominal ultrasonography were all unremarkable. Targeted NGS performed on affected tissue identified a *PIK3CA* (NM_006218.4) variant, c.3140A>G (p.His1047Arg), with a VAF of 2% and a read depth of 1088× (Fig. 2c). In accordance with ACMG/AMP guidelines, this

missense variant satisfied the criteria PS3, PS4, PM1, PM2, and PM5, and was consequently classified as pathogenic.

Patient 4

A 4-year-old female was referred to our clinic for evaluation of hemihypertrophy. Her prenatal history was normal. She was born at 39 weeks of gestation via spontaneous vaginal delivery, weighing 3750 g. After birth, she was admitted to an incubator for 8 days due to pneumonia.

Her developmental milestones were appropriate for age. She was the first child of a non-consanguineous 25-year-old healthy mother and a 28-year-old healthy father. On physical examination, her weight was 19 kg (0.36 SDS), height was 115 cm (1.51 SDS), and head circumference was 53 cm (1.63 SDS). She had no obvious dysmorphic features, but facial asymmetry was noted (Fig. 1f). Dryness of the skin was present on the upper extremities and abdomen, and bilateral diffuse capillary hemangiomas were observed on the lower extremities. Additionally, the second and third toes of the left foot were enlarged compared with the contralateral side (Fig. 1g). Investigations including echocardiography, abdominal ultrasonography, MLPA analysis for Beckwith-Wiedemann syndrome (BWS), and clinical exome sequencing were unremarkable. Targeted NGS performed on affected tissue identified a *PIK3CA* (NM_006218.4) variant, c.2176G>A (p.Glu726Lys), with a VAF of 3.47% and a read depth of 1645 (Fig. 2d). According to ACMG/AMP guidelines, this missense variant met the PS2, PS4, PM1, PM2, PP2 criteria and was classified as pathogenic.

Patient 5

A 7-year-old male with an initial clinical impression of Sturge-Weber syndrome was referred to our clinic. He was born at term via cesarean section, weighing 2850 g, as the second child of non-consanguineous parents.

He had two healthy siblings, and his prenatal, postnatal and family histories were unremarkable. At presentation, physical examination revealed mild facial erythema, a port-wine stain on the left side of the face, a slightly narrow palate, reddish-brown discoloration of the abdomen, vascular malformations on the right extremity (Fig. 1h) and on the left lateral side of neck and a 5 × 5 cm subcutaneous soft-tissue swelling in the right lumbar region (Fig. 1i). Bilateral pes planus and hand-foot anomalies were also noted. His weight was 28 kg (1.14 SDS), height was 129 cm (1.26 SDS) and head circumference was 50 cm (-1.45 SDS). The patient had no hearing loss, learning difficulties, scoliosis, or pectus excavatum. Fundoscopic examination revealed only grade 1-2 papillary edema. Superficial ultrasonography of the lumbar region demonstrated localized skin thickening and edematous subcutaneous tissue. Brain MRI and echocardiography were unremarkable, while the bone survey showed mild patellar irregularity. Abdominal ultrasonography demonstrated hepatomegaly. A skin biopsy from the affected area was obtained and analyzed for *PIK3CA* mutation to confirm the diagnosis. Targeted NGS identified a *PIK3CA* (NM_006218.4) variant, c.2740G>A (p.Gly914Arg), with a VAF of 9% and a read depth of 1238 (Fig. 2e). According to ACMG/AMP guidelines, this missense variant met the criteria PS2, PS4, PM2, PM1, PP2, and PP3 criteria and was classified as pathogenic.



Figure 1. Clinical photographs of patients with *PIK3CA*-related overgrowth spectrum (PROS) illustrating the characteristic mosaic pattern of segmental overgrowth and vascular anomalies. **(a)** Patient 1 demonstrates prominent surface veins and right-sided upper limb overgrowth. **(b)** Dilated veins on the right lower leg and bilateral macrodactyly of the second toes are observed. **(c)** A hemangiomatous lesion is visible on the plantar surface of the right foot. **(d)** Patient 2 presents with facial asymmetry due to a soft, mobile 2 cm mass on the left cheek. **(e)** Multiple cutaneous hemangiomas and soft-tissue overgrowth are noted on the back. **(f)** Patient 4 exhibits facial asymmetry. **(g)** Macrodactyly involving the second and third toes of the left foot is evident. **(h)** Patient 5 shows a hyperpigmented patch on the posterior aspect of the right leg. **(i)** Patient 5 demonstrates localized soft-tissue hypertrophy in the right lumbar region.

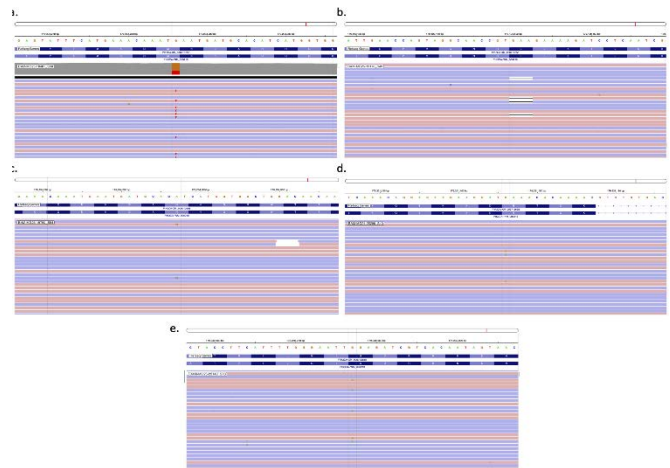


Figure 2. Integrative Genomics Viewer (IGV) screenshots showing the identified *PIK3CA* variants in the five patients with *PIK3CA*-related overgrowth spectrum (PROS). **(a)** Patient 1: c.3129G>T (p.Met1043Ile), variant allele frequency (VAF) 3%, read depth 1071x. **(b)** Patient 2: c.328_330del (p.Glu110del), VAF 5%, read depth 836x. **(c)** Patient 3: c.3140A>G (p.His1047Arg), VAF 2%, read depth 1088x. **(d)** Patient 4: c.2176G>A (p.Glu726Lys), VAF 3.47%, read depth 1645x. **(e)** Patient 5: c.2740G>A (p.Gly914Arg), VAF 9%, read depth 1238x.

Each variant is highlighted in the sequencing reads aligned to the *PIK3CA* (NM_006218.4) reference transcript.

Clinical and molecular findings of the five patients with *PIK3CA*-related overgrowth spectrum (PROS) are summarized in Table 1.

Table 1: Clinical and molecular findings of five patients with *PIK3CA*-related overgrowth spectrum (PROS). The table summarizes the main clinical characteristics and molecular analysis results of the patients. All five patients exhibited typical features characterized by segmental overgrowth and/or vascular malformations.

	Sex	Main Clinical features	Variants	VAF	Sequencing depth	PROS Subtype	Sequencing on peripheral blood
Patient 1	Female	Right-sided segmental overgrowth, port-wine stain, scoliosis, hepatomegaly	c.3129G>T p.Met1043Ile rs121913283	%3	1071	KTWS	negative
Patient 2	Male	Congenital lymphatic and vascular malformations, multiple hemangiomas, facial asymmetry, ASD	c.328_330del p.Glu110del	%5	836	CLOVES	NA
Patient 3	Female	Macrodactyly, soft-tissue hypertrophy, pectus excavatum, joint laxity	c.3140A>G p.His1047Arg rs121913279	%2	1088	KTWS	negative
Patient 4	Female	Hemihypertrophy, facial asymmetry, capillary hemangiomas, skin dryness	c.2176G>A p.Glu726Lys rs867262025	%3.47	1645	KTWS	NA
Patient 5	Male	Segmental overgrowth, vascular malformations, soft-tissue hypertrophy, hepatomegaly, port-wine stain	c.2740G>A p.Gly914Arg rs587776932	%9	1238	CLOVES	NA

Targeted next-generation sequencing (NGS) performed on affected tissue identified somatic *PIK3CA* variants with low variant allele frequencies, consistent with mosaicism. All variants were classified as pathogenic according to ACMG/AMP guidelines based on supporting evidence. Abbreviations: ASD, atrial septal defect; VAF, variant allele frequency, NA: Not applicable, CLOVES: Congenital Lipomatous Overgrowth, Vascular malformations, Epidermal nevi, and Spinal/skeletal anomalies and/or scoliosis, KTWS: Klippel–Trenaunay–Weber syndrome

DISCUSSION

The present study describes five patients with clinical and molecularly confirmed *PIK3CA*-related overgrowth spectrum (PROS), each harboring somatic mosaic *PIK3CA* variants detected in affected tissue. Despite their heterogeneous presentations, all patients demonstrated the hallmark features of PROS, including segmental overgrowth, vascular and lymphatic malformations and cutaneous involvement. The identification of distinct pathogenic variants distributed across multiple functional domains of the *PIK3CA* protein further underscores the phenotypic and genotypic diversity within this spectrum. This case series adds to the expanding evidence that implicates *PIK3CA* mosaicism in localized overgrowth disorders and underscores the significance of combining clinical, radiologic,

and molecular data for precise diagnosis and effective management. Gain-of-function (GOF) variants in the *PIK3CA* gene are now recognized as the molecular basis of a group of clinically overlapping mosaic overgrowth disorders collectively termed the PROS⁴⁻⁶. Disorders included within this spectrum encompass CLOVES syndrome (Congenital Lipomatous Overgrowth, Vascular malformations, Spinal/Skeletal anomalies), Megalencephaly–Capillary Malformation syndrome (MCAP), Epidermal nevi, Fibroadipose Hyperplasia (FAH), Isolated Macrodactyly, Hemihyperplasia–Multiple Lipomatosis (HHML), Congenital Lipomatous Overgrowth without Skeletal anomalies and Diffuse Capillary Malformation with Overgrowth (DCMO)^{4,7}. The underlying mechanism involves hyperactivation of the PI3K/AKT/mTOR

signaling pathway, leading to dysregulated cell growth, proliferation and vasculogenesis.

Although the Online Mendelian Inheritance in Man (OMIM) database does not yet explicitly define an association between *PIK3CA* variants and KTWS, accumulating molecular and phenotypic evidence supports its inclusion within the PROS continuum⁸. The characteristic manifestations of KTWS—segmental overgrowth, capillary, venous, and lymphatic malformations, along with soft-tissue and skeletal hypertrophy—closely correspond to the clinical features observed in PROS.

The diagnosis of PROS relies on the combined assessment of clinical and molecular criteria. Clinically and molecularly, the defining features include (i) congenital or early-onset segmental or mosaic-patterned overgrowth, (ii) the presence of vascular malformations that may be capillary, venous, or lymphatic, and (iii) detection of a pathogenic *PIK3CA* variant in affected tissue, usually at a low variant allele frequency indicative of mosaicism^{2,9}. These criteria are particularly important because *PIK3CA* mosaic variants are often confined to affected tissues and may not be detectable in DNA derived from peripheral blood. In our cohort, blood samples were analyzed only for Patients 1 and 3, and the variants identified in affected tissue were not detected in leukocyte-derived DNA, further supporting the presence of somatic mosaicism. Although patients with PROS exhibit substantial phenotypic heterogeneity, they can be broadly classified under the PROS umbrella. Based on clinical presentation, three patients in our series demonstrated features consistent with KTWS, whereas two patients exhibited findings compatible with CLOVES syndrome.

Among the five *PIK3CA* variants identified in our cohort, four were clustered within the C-terminal region (Fig. 3), encompassing the helical and kinase domains, which represent well-established mutational hotspots of the

protein. This finding is consistent with previous reports, as all identified variants have been previously described in association with cancer and PROS cases. Only one variant identified in our study (p.Glu110del) was located in the N-terminal adaptor-binding (PI3K-ABD) domain of the protein or gene. Of the five identified *PIK3CA* variants in our cohort, four were missense substitutions, consistent with the predominance of activating missense changes reported in PROS, while one patient carried an in-frame deletion. The p.Glu110del variant has previously been described in individuals with lymphatic malformations and KTWS, as well as in a CLOVES case within a larger cohort, consistent with the phenotype observed in our Patient 2¹⁰⁻¹². This observation further supports the role of the *PIK3CA* p.Glu110del variant as a recurrent pathogenic change associated with mixed vascular-adipose overgrowth phenotypes across the PROS spectrum. The p.Met1043Ile variant has been previously reported predominantly in patients with PROS presenting with hemimegalencephaly or megalencephaly phenotypes³. In contrast, our Patient 1, who harbored the same variant, exhibited clinical features consistent with KTWS. This observation highlights the broad phenotypic heterogeneity associated with *PIK3CA* activating variants, even among individuals carrying identical hotspot mutations. The His1047, together with Glu542 and Glu545, accounts for more than 80% of all reported variants in patients with PROS^{6,13,14}. The His1047Arg variant is the most frequently observed substitution in the COSMIC database and is known to confer a strong oncogenic activation of the PI3K pathway. Consistent with the findings reported by Kuentz et al., our Patient 3 carrying this variant did not present with any brain anomalies³. The Glu726Lys variant, identified in Patient 4, has also been previously reported in association with KTWS, consistent with the findings of Gokpınar Ili et al.¹⁵. Our patient additionally exhibited facial

asymmetry, expanding the phenotypic spectrum associated with this variant. This observation supports the pathogenic relevance of this missense variant within the PROS spectrum and its recurring link to vascular malformations and segmental overgrowth phenotypes characteristic of KTWS. In a Korean MCAP cohort, the Gly914Arg variant was identified as the most frequent alteration, detected in four patients. Among these, two exhibited megalencephaly, one had polydactyly, and one presented with Arnold–Chiari type I malformation; however, none of these features were observed in our patient. However, cutaneous facial vascular malformations, reported in three of the four Korean cases, were also present in our patient, supporting a partial phenotypic overlap¹⁶.



Figure 3. Schematic representation of the PIK3CA protein illustrating its major functional domains from the N-terminal to the C-terminal. The domains include PI3K-ABD (residues 16–105), PI3K-RBD (187–289), C2 PI3K-type (330–487), PIK helical (517–694), and PI3K/PI4K catalytic (765–1051). The identified variants from the five patients in this study are mapped onto the corresponding domains: p.Glu110del, p.Glu726Lys, p.Gly914Arg, p.Met1043Ile, and p.His1047Arg. Each variant is indicated at its respective position along the protein structure.

The identified variants had an average sequencing depth of approximately 1100×, with the lowest VAF detected at 2%, and no correlation between disease severity and VAF was observed, consistent with previous reports. This observation supports the notion that the severity of clinical manifestations is more closely related to the timing of the mutational event during development and the specific tissues affected, rather than the absolute allele frequency of the variant. We believe that even variants with low variant allele frequencies

should be reported, particularly when there is strong clinical correlation and when the variant represents a recurrently observed alteration in previously documented cases.

We propose that, although we categorized PROS into subtypes based on the patients’ clinical presentations as summarized in Table 1, this group of disorders should ultimately be regarded under a single overarching entity within the PROS framework, as the clinical manifestations among subtypes are highly intertwined and clear diagnostic boundaries have not been fully established yet.

Recent studies have demonstrated highly favorable outcomes with Alpelisib, an FDA-approved agent for the treatment of PROS in both pediatric and adult patients¹⁷. We consider case-based reports such as the present study to be of great importance in raising awareness among medical geneticists, thereby promoting early diagnosis and appropriate management of affected individuals. Furthermore, given its demonstrated efficacy, broader access to Alpelisib therapy through national reimbursement policies in Türkiye may contribute to improved clinical outcomes and quality of life for patients with PROS. Given the expanding therapeutic landscape, molecular confirmation of PROS serves not only as a diagnostic tool but also as a critical determinant in therapeutic decision-making and clinical management.

Ethical approval: All procedures performed in this study were in accordance with the ethical standards specified in the World Medical Association Declaration of Helsinki. Ethical committee approval for the study was obtained from Ankara Etlik City Hospital Ethical Board on 17 Dec 2025 (No: AEŞH-BADEK1-2025-606).

Conflict of Interest: The authors declared no conflicts of interest.

Financial Disclosure: The authors declared that this study has received no financial support.

REFERENCES

1. Mirzaa G, Graham JM Jr, Keppler-Noreuil K. PIK3CA-Related Overgrowth Spectrum. In: GeneReviews®. University of Washington, Seattle, Seattle (WA); 1993. PMID: 23946963.
2. Keppler-Noreuil KM, Rios JJ, Parker VE, et al. PIK3CA-related overgrowth spectrum (PROS): diagnostic and testing eligibility criteria, differential diagnosis, and evaluation. *Am J Med Genet A*. 2015;167A(2):287-95.
3. Kuentz P, St-Onge J, Duffourd Y, et al. Molecular diagnosis of PIK3CA-related overgrowth spectrum (PROS) in 162 patients and recommendations for genetic testing. *Genet Med*. 2017;19(9):989-97.
4. Lindhurst MJ, Parker VE, Payne F, et al. Mosaic overgrowth with fibroadipose hyperplasia is caused by somatic activating mutations in PIK3CA. *Nat Genet*. 2012;44(8):928-33.
5. Keppler-Noreuil KM, Sapp JC, Lindhurst MJ, et al. Clinical delineation and natural history of the PIK3CA-related overgrowth spectrum. *Am J Med Genet A*. 2014;164A(7):1713-33.
6. Mirzaa G, Timms AE, Conti V, et al. PIK3CA-associated developmental disorders exhibit distinct classes of mutations with variable expression and tissue distribution. *JCI Insight*. 2016;1(9):e87623.
7. Sapp JC, Turner JT, van de Kamp JM, et al. Newly delineated syndrome of congenital lipomatous overgrowth, vascular malformations, and epidermal nevi (CLOVE syndrome) in seven patients. *Am J Med Genet A*. 2007;143A(24):2944-58.
8. Sasaki Y, Ishikawa K, Hatanaka KC, et al. Targeted next-generation sequencing for detection of PIK3CA mutations in archival tissues from patients with Klippel-Trenaunay syndrome in an Asian population : List the full names and institutional addresses for all authors. *Orphanet J Rare Dis*. 2023;18(1):270.
9. Yeung KS, Ip JJ, Chow CP, et al. Somatic PIK3CA mutations in seven patients with PIK3CA-related overgrowth spectrum. *Am J Med Genet A*. 2017;173(4):978-84.
10. Brouillard P, Schlögel MJ, Homayun Sepehr N, et al. Non-hotspot PIK3CA mutations are more frequent in CLOVES than in common or combined lymphatic malformations. *Orphanet J Rare Dis*. 2021;16(1):267.
11. Zhang B, He R, Xu Z, et al. Somatic mutation spectrum of a Chinese cohort of pediatrics with vascular malformations. *Orphanet J Rare Dis*. 2023;18(1):261.
12. Keppler-Noreuil KM, Lozier J, Oden N, et al. Thrombosis risk factors in PIK3CA-related overgrowth spectrum and Proteus syndrome. *Am J Med Genet C Semin Med Genet*. 2019;181(4):571-81.
13. Madsen RR, Vanhaesebroeck B, Semple RK. Cancer-Associated PIK3CA Mutations in Overgrowth Disorders. *Trends Mol Med*. 2018;24(10):856-70.
14. Mussa A, Leoni C, Iacoviello M, et al. Genotypes and phenotypes heterogeneity in PIK3CA-related overgrowth spectrum and overlapping conditions: 150 novel patients and systematic review of 1007 patients with PIK3CA pathogenetic variants. *J Med Genet*. 2023;60(2):16373.
15. Gökpınar İli E, Taşdelen E, Durmaz CD, et al. Phenotypic and molecular characterization of five patients with PIK3CA-related overgrowth spectrum (PROS). *Am J Med Genet A*. 2022;188(6):1792-800.
16. Park HJ, Shin CH, Yoo WJ, et al. Detailed analysis of phenotypes and genotypes in megalencephaly-capillary malformation-polymicrogyria syndrome caused by somatic mosaicism of PIK3CA mutations. *Orphanet J Rare Dis*. 2020;15(1):205.
17. Canaud G, Lopez Gutierrez JC, Irvine AD, et al. Alpelisib for treatment of patients with PIK3CA-related overgrowth spectrum (PROS). *Genet Med*. 2023;25(12):100969.